Hall-B Tagger Absolute Energy Calibration

Itaru Nakagawa
University of Kentucky

January 30, 2004

Abstract

The method to calibrate the absolute photon energy of the Hall-B tagger is studied. The actual calibration is done by sending primary electron, which energy is know to 10^{-4} directly into the tagger and observe a firing E-counter. The major worry of the radiation damage of the vacuum Mylar and high counting rate in the scintillator can be eased by reducing the peak current using the collimating defocused beam. The feasibility of this method is discussed in the document.

1 Collimation of Defocused Beam

It has been a long standing issue to calibrate the absolute energy of the Hall-B tagger. Sending primary electron beam with known absolute energy directly to the tagger is one of the method to do so. However, it has been hesitated primarily because of following two reasons. 1) Too high counting rates in a single scintillator and 2) a possible radiation damage in the vacuum Mylar window even with the lowest current (in the order of 100 pA) the accelerator can deliver within a comfortable control of the beam. At the current of 100 pA order, many beam monitoring devices start to loose the sensitivity to the current and tuning the beam without reliable beam monitor informations makes this method unpractical. In order to perform the calibration satisfactory, the delivered beam to the tagger has to be under control within the tolerant level for the tagger to function as a 10^3 precision device as it is originally designed. In other word, the calibration becomes feasible once the way to deliver well controlled but somewhat reduced current beam to the tagger, since the high counting rate is the primary worry for the calibration. Here is one of the technique I propose to reduce the peak current of the beam. The peak current is drastically reduced by collimating the (intentionally) defocused beam at the collimator. The schematic image of the concept is illustrated in Figure. 1. The primary beam is strongly defocused at the upstream of the tagger. The collimator is thick enough to block any current except for the small portion of the beam go through a central collimation hole. The reduced beam current passed the collimator is then transported into the tagger. The scintillator E-counter whichever fires

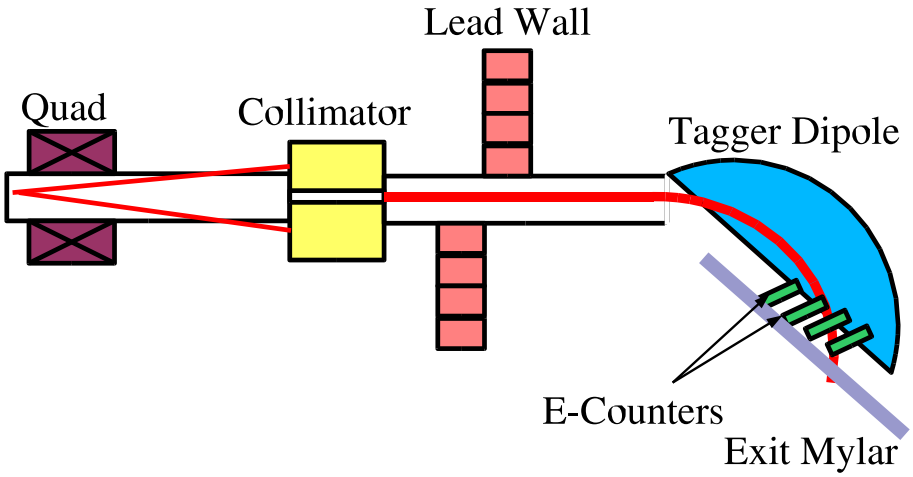

Figure 1: Schematic diagram of the setup. The primary beam is intentionally defocused using existing quadrupoles on the Hall-B beam line and collimated by a collimator to reduce the peak current. A small current after the collimator then transported into the Hall-B tagger. The radiator is not used, since the primary electron beam is used for the calibration.

should tell us the photon energy. Since the primary electron beam with known beam energy is used for the calibration, the radiator is kept away from the beam line.

In order to make this technique feasible, several technical/safety aspects have to be satisfied. Major items are

- Beam quality after the collimation
- Radiation damage of the exit Mylar
- Large beam spot size tuning
- Machining collimator within certain precision
- Radiation Safety

Some of above items are discussed in the later sections. In the following section, the requirement of the collimator design is discussed. The design of the collimator should be constrained by the beam characteristics accepted by the optical property of the tagger.

2 Collimated Beam Requirement

2.1 Beam Spot Size and Angular Dispersion

The major property of the collimator needs to be optimized by accounting the entry beam requirement of the tagger so that the collimated beam characteristic still satisfies 0.1% intrinsic resolution of the tagger. For instance, the radius and length of the collimator supposed to be constrained by the geometrical and angular allowances of the tagger to function as of 0.1 % level resolution, respectively. The energy resolution is ultimately determined by the beam spread size at the focal plane. The estimation is done using the first order transport coefficients from Table III of reference[1]. For given beam spot and angular spread ($\sigma_{\rm x}$ and σ_θ, respectively), the energy resolution of post bremsstrahlung electrons $\Delta p_{\rm e}/p_{\rm e} \times 100$ [%] is calculated by following formula:

$$\frac{\Delta p_{\rm e}}{p_{\rm e}} \times 100 = \frac{\sigma_{\rm x} R_{11}}{10 R_{16}} \quad (1)$$

$$\frac{\Delta p_{\rm e}}{p_{\rm e}} \times 100 = \frac{\sigma_\theta R_{11}}{10 R_{16}} \quad (2)$$

where R_{ij} denotes for transport matrix element[2] and detailed explanations are

R_{11} : $(x|x)$ from radiator to detector plane [mm/mm]
R_{12} : $(x|\theta)$ from radiator to detector plane [mm/mrad]
R_{16} : $(x|p)$ from radiator to detector plane [cm/%].

The factor 10 appears in the denominator of Equations (1) and (2) is an unit conversion factor between mm and cm. The energy resolution of the post bremsstrahlung electron energy is then translated into that of a tagged photon $\Delta k/k$ using a following relation;

$$k = E_0 - p_{\rm e} \quad (3)$$

where E_0 is the primary electron beam energy. Taking differential of Equation (4),

$$\Delta k = -\Delta p_{\rm e} \quad (4)$$

$$\frac{\Delta k}{k} = -\frac{\Delta p_{\rm e}}{k} = -\frac{p_{\rm e}}{k}\frac{\Delta p_{\rm e}}{p_{\rm e}} \quad (5)$$

where $\Delta p_{\rm e}/p_{\rm e}$ is given from Equations (1) and (2). The energy resolutions for tagged photon energy are studied for $\sigma_{\rm x} = (0.25, 0.5, 1.0)$ mm and $\sigma_\theta = (10, 20, 30)$ mrad cases. Calculated results are tabulated in Tables 1 and 2.

[1] Dan Sober, CLAS-Note 91-012
[2] See Karl L. Brown, SLAC-75 report for notations.

Table 1: Energy resolutions of post-bremsstrahlung electrons and tagged photons depending on the beam spread σ_x at the entrance of the tagger.

			σ_x [mm]	0.25	0.5	1	0.25	0.5	1
k/E_0	p_e/k	R_{11} [mm/mm]	R_{16} [cm/%]	$\Delta p_e/p_e$ [%]	$\Delta p_e/p_e$ [%]	$\Delta p_e/p_e$ [%]	$\Delta k/k$ [%]	$\Delta k/k$ [%]	$\Delta k/k$ [%]
0.95	0.053	-0.72	0.31	-0.06	-0.12	-0.23	0.00	-0.01	-0.01
0.90	0.111	-0.72	0.41	-0.04	-0.09	-0.18	0.00	-0.01	-0.02
0.80	0.250	-0.79	0.58	-0.03	-0.07	-0.14	-0.01	-0.02	-0.03
0.70	0.429	-0.83	0.75	-0.03	-0.06	-0.11	-0.01	-0.02	-0.05
0.60	0.667	-0.86	0.91	-0.02	-0.05	-0.09	-0.02	-0.03	-0.06
0.50	1.000	-0.89	1.07	-0.02	-0.04	-0.08	-0.02	-0.04	-0.08
0.40	1.500	-0.91	1.23	-0.02	-0.04	-0.07	-0.03	-0.06	-0.11
0.30	2.333	-0.92	1.39	-0.02	-0.03	-0.07	-0.04	-0.08	-0.15
0.20	4.000	-0.93	1.55	-0.01	-0.03	-0.06	-0.06	-0.12	-0.24

Table 2: Energy resolutions of post-bremsstrahlung electrons and tagged photons depending on the beam angular spread σ_θ at the entrance of the tagger.

			σ_θ [mrad]	10	20	30	10	20	30
k/E_0	p_e/k	R_{12} [mm/mr]	R_{16} [cm/%]	$\Delta p_e/p_e$ [%]	$\Delta p_e/p_e$ [%]	$\Delta p_e/p_e$ [%]	$\Delta k/k$ [%]	$\Delta k/k$ [%]	$\Delta k/k$ [%]
0.95	0.053	-0.134	0.31	-0.435	-0.870	-1.305	-0.023	-0.046	-0.069
0.90	0.111	-0.055	0.41	-0.136	-0.272	-0.407	-0.015	-0.030	-0.045
0.80	0.250	-0.010	0.58	-0.017	-0.034	-0.052	-0.004	-0.009	-0.013
0.70	0.429	0.003	0.75	0.004	0.008	0.012	0.002	0.003	0.005
0.60	0.667	0.007	0.91	0.008	0.015	0.023	0.005	0.010	0.015
0.50	1.000	0.006	1.07	0.006	0.011	0.017	0.006	0.011	0.017
0.40	1.500	0.003	1.23	0.002	0.005	0.007	0.004	0.007	0.011
0.30	2.333	-0.002	1.39	-0.001	-0.003	-0.004	-0.003	-0.007	-0.010
0.20	4.000	-0.007	1.55	-0.005	-0.009	-0.014	-0.018	-0.036	-0.054

2.2 Beam Current

In this section, the beam current reduction efficiency as a function of a collimator diameter is studied. In addition to 0.1% energy resolution limit of the tagger as discussed in the previous subsection, the collimator diameter is also constrained for the maximum beam current tolerance of the tagger scintillators and the vacuum Mylar. The latter issue is raised from the radiation damage. As studied more detail in Section 6, it is likely that the beam current which is argued here is low enough to see the serious radiation damage in the Mylar. Thus the beam current requirement is simply estimated from the maximum counting rate can be handled by a tagger scintillator. The current operational limit of the tagger scintillators are approximately 1 MHz per T-counter. This limit comes rather from the dead time of the data acquisition system. For the energy calibration purpose, the dead time is not a serious problem, since the energy calibration can be done simply by observing which scintillator is fired. Thus the goal of reduced counting rate is set to a few to several MHz in a single E-counter here, which is considered to be a safety operation level for photo tubes. Note that the measurement can be done within very short time and photo tubes can be operated with lowered high voltages for safety.

In the Table 3, collimated beam current I_c is calculated depending on collimator diameter ϕ (radius $r = \phi/2$). Initial electron beam $I_c = 100$ pA and defocused beam spot size $\sigma_x^0 = 5$ mm is assumed in front of the collimator. The existing beam pipe has diameter of 21 mm (radius 10.5 mm), which corresponds to about 2σ away from the $\sigma_x^0 = 5$ mm beam spread. About $(1 - 0.95^2) \times 100 = 10\%$ of the incident electrons (10 pA of 100 pA beam) will hit the beam pipe upstream of the collimator. Reduction (collimation rate) is calculated by squaring Gaussian integral probability function for $\sigma = r/\sigma_x^0$.

Table 3: The collimated beam current I_c and counting rate for various collimator diameters ϕ assuming initial beam current of $I_0 = 100$ pA and beam spot size $\sigma_x^0 = 5$ mm at the front of the collimator.

ϕ [mm]	r [mm]	r/σ_x^0	Reduction [%]	I_c	Rates
2	1	0.2	2.5	2 pA	15 MHz
1	0.5	0.1	0.64	500 fA	4 MHz
0.5	0.25	0.05	0.16	160 fA	1 MHz

As can be seen from the table, a few MHz counting rate can be achieved by $\phi \sim 1$ mm diameter collimator with defocused beam spot size of $\sigma_x^0 = 5$ mm and beam current of $I_0 = 100$ pA. The feasibility of tuning such the beam is discussed by the accelerator devision of JLab[3]

[3]private communication with Hari Areti, Jay Benesch, and Johan Bengtsson.

3 Collimator Design

A current collimator design is illustrated in Figure.2. Two tungstate plates with half of the collimator hole machined in each at the center of plates and slide perpendicularly to the beam axis. The collimator hole remains at the beam center when plats are closed. This design has advantage in machining such a small hole in a good precision.

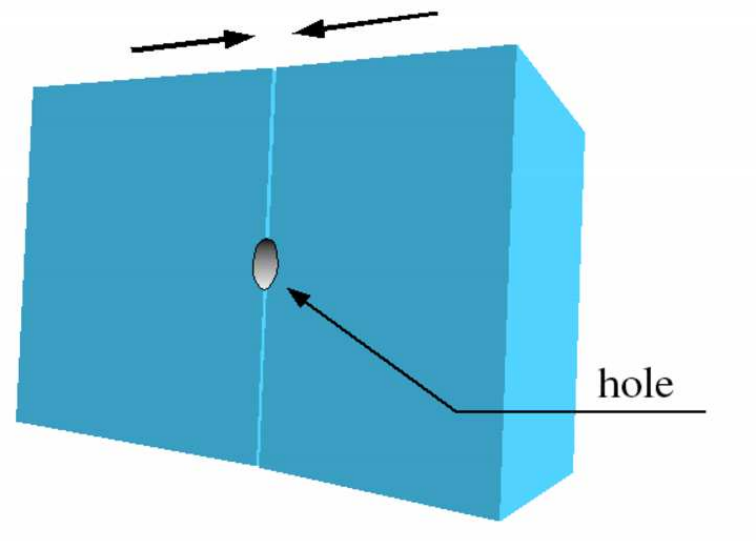

Figure 2: A design of the collimator. Two sliding tungstate collimator with half of the hole machined in each at the center.

The thickness of the collimator has to be optimized by accounting radiation length for the incident electron and an angular collimation of the beam. As presented in Table 2, the angular tolerance σ_θ for the collimated beam requirement is 10 to 20 mrad to achieve the 0.1% energy resolution of the tagged photon. The relation between the thickness of the collimator and the angular collimation σ_θ of the beam and radiation length are tabulated in Table. 4 for the diameter of collimator $\phi = 0.5, 1, 2$ mm cases. Note the satisfactory radiation length of the collimator is comparable to the angular tolerance σ_θ.

4 Collimator Location

Two feasible locations are indicated by brown arrows in the Figure 3. The figure is the schematic diagram of the latest beam line apparatus upstream of the Hall-B tagger. The feasible locations are 1) between the Moller Quadrupoles and the Q-Q-Q triplet and 2) between the Q-Q-Q triplet and the tagger. The advantage of 1) is that the collimation is done before the existing lead wall shielding before the tagger. For radiation shielding purpose. this is preferable. The location 2) is actually behind the lead wall. However, the advantage of 2) is relatively simple manner to enlarge the beam spot. In order to obtain

Table 4: The relation between the thickness of the collimator and the angular collimation σ_θ of the beam and radiation length for the diameter of collimator $\phi = 0.5, 1, 2$ mm cases.

thickness t [cm]	ϕ [mm]	σ_θ [mrad]	$t/X_{\rm rad}$
5	0.5	10	14
5	1	20	14
5	2	40	14
10	1	10	28
10	2	20	28

$\sigma_{\rm x}^0 = 5$ mm beam spot size, the Q-Q-Q triplet can play a primary roll and in consequence, the number of quadrupole magnets to be involved can be reduced.

5 Large Beam Spot Simulation

In this section, the feasibility of the enlarging beam spot size is studied To conclude from the study, it is feasible to make the beam spot size greater than 1 cm using exisiting several quadrupole magnets installed in hall-B beam line upstream the tagger, although the initial beam spot size is in the order of 100 μm. The study[4] was performed using the beam transport simulation program OPTIM[5]. The result of the study is plotted in the figure4. The holizontal (red) and vertical (green) curves represents the simulated beam spot size plotted as a function of the distance from the hall-B beam line. The distance scale is given in meter. Several quadrupoles along the beam line are involved to enlarge the beam spot. The beam spot size of about 1 cm is achieved within practical currents in the quadrupole magnets[6].

6 Radiation Damage of Vacuum Mylar

This study was made based on the previous report[7]. It reports the Mylar starts to show damage at the radiation doses of 10^7 [Rad].

For collimated beam spot size of $\sigma_{\rm x} \times \sigma_{\rm y} = 1 \times 1$ mm^2 case, for instance, the intercepting area of the beam of the vacuum window is about 4 mm^2 because the beam intercepts the window at a very oblique angle of 15°. Using the ionization loss of relativistic particle in Mylar 1.8 MeV cm^2/g/cm^2, the dose given to the window per electron, $D_{\rm we}$ is

[4] private communication with Jay Benesch

[5] written by Valeri Lebedev.

[6] The maximum current limit for Moller quads are not confirmed

[7] Hall Crannel, *1 Radiation dose due to beam on the Tagger Window in Hall-B*

$$D_{\rm we} = \frac{1.8[{\rm MeVcm^2/g/cm^2}]}{4\times10^{-2}[{\rm cm^2}]}\frac{100[{\rm Rad}]}{6.24\times10^{9}[{\rm MeV/g}]} \sim 7.2\times10^{-7}[{\rm Rad/e}] \quad (6)$$

For collimated beam current of $I_{\rm c} = 1$ pA, which corresponds to 6 MHz electrons intercepts the Mylar, the radiation dose rate is calculated to be 4.3 Rad/s. To be 1 % of the damaging does threshould 10^7 [Rad], the exposure time allowed is 2.3×10^4 sec (6.4 hours). The single calibration can be done within 10 sec, and which is short enough not to damage the Mylar due to the radiation.

7 Measurement

The actual calibration is preferred to be done with two different beam energies 0.8 and 1.6 GeV for the sake of cross checks. The red and blue curves in the Figure 5 indicate the field setting of primary electron energy E_0 dependence of the focal plane for post bremsstrahlung electron energies of $p_{\rm e}$=0.8 and 1.6 GeV, respectively. Since this calibration is to run without the bremsstrahlung target, $p_{\rm e}$ represents actually the primary electron beam energy, in this case. Plotted with solid circles are proposed measurement points. The primary energy of 0.8 and 1.6 measurements presumably be able to cover 20 % to 86 % and 20 % to 78 % of the focal plane momentum range, respectively. Unfortunately, the magnetic field setting for the tagger magnet get too high beyond these ranges and therefore not feasible to perform the calibration with these primary energies.

8 Acknowledgment

I thank Dan Sober (The Catholic University of America) for the calculation of the beam characteristic requirements of the tagger. I acknowledge Hall Crannel (The Catholic University of America) for the radiation dose estimation of the Mylar. I thank Hari Areti, Jay Benesch, and Johan Bengtsson (Accelerator division of Jlab) for educating me the basics of the accelerator physics and the study of the defocused beam tuning.

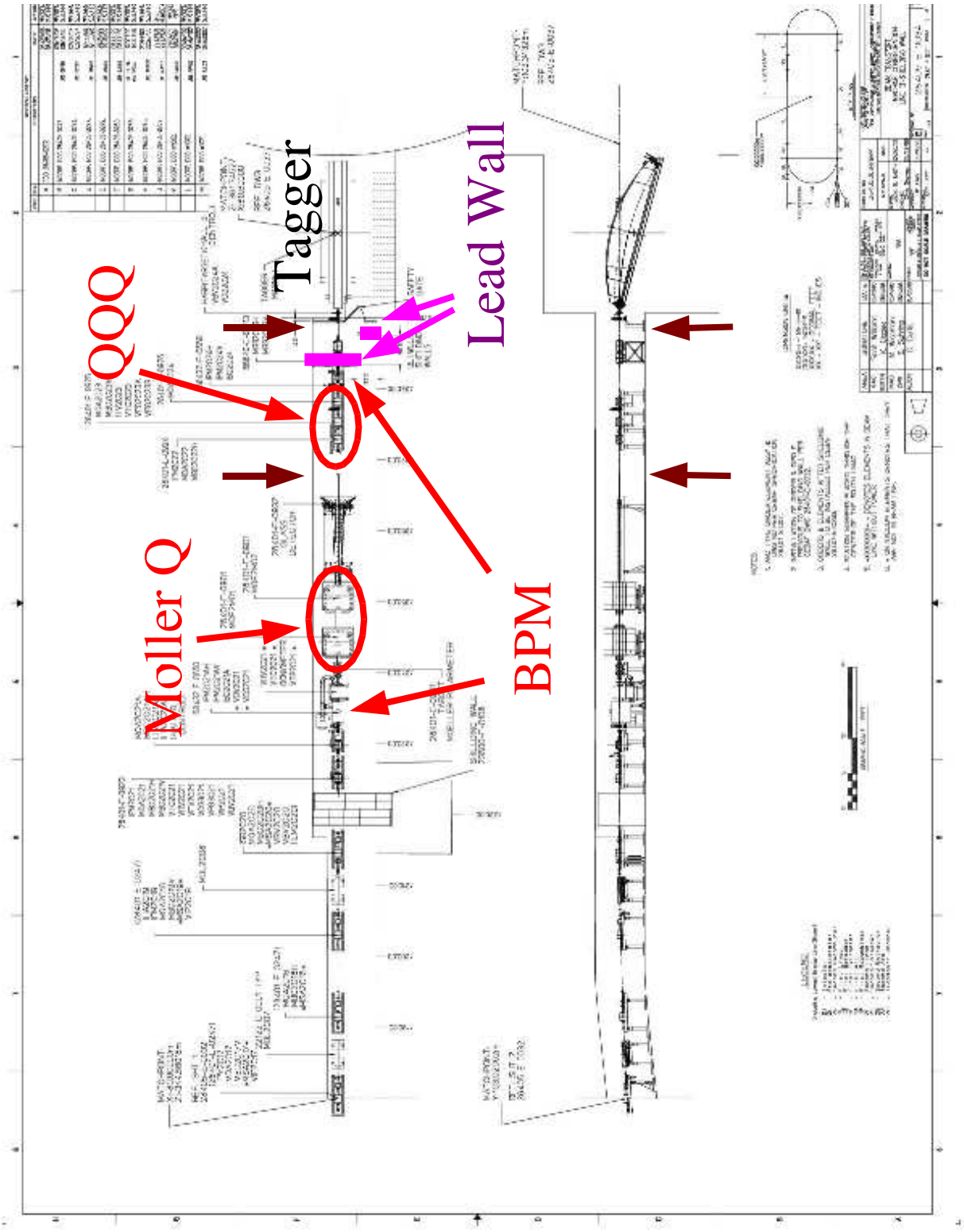

Figure 3: Schematic diagram of the Hall-B beam line upstream of the tagger. Feasible locations for the collimator to be installed are indicated by brown arrows.

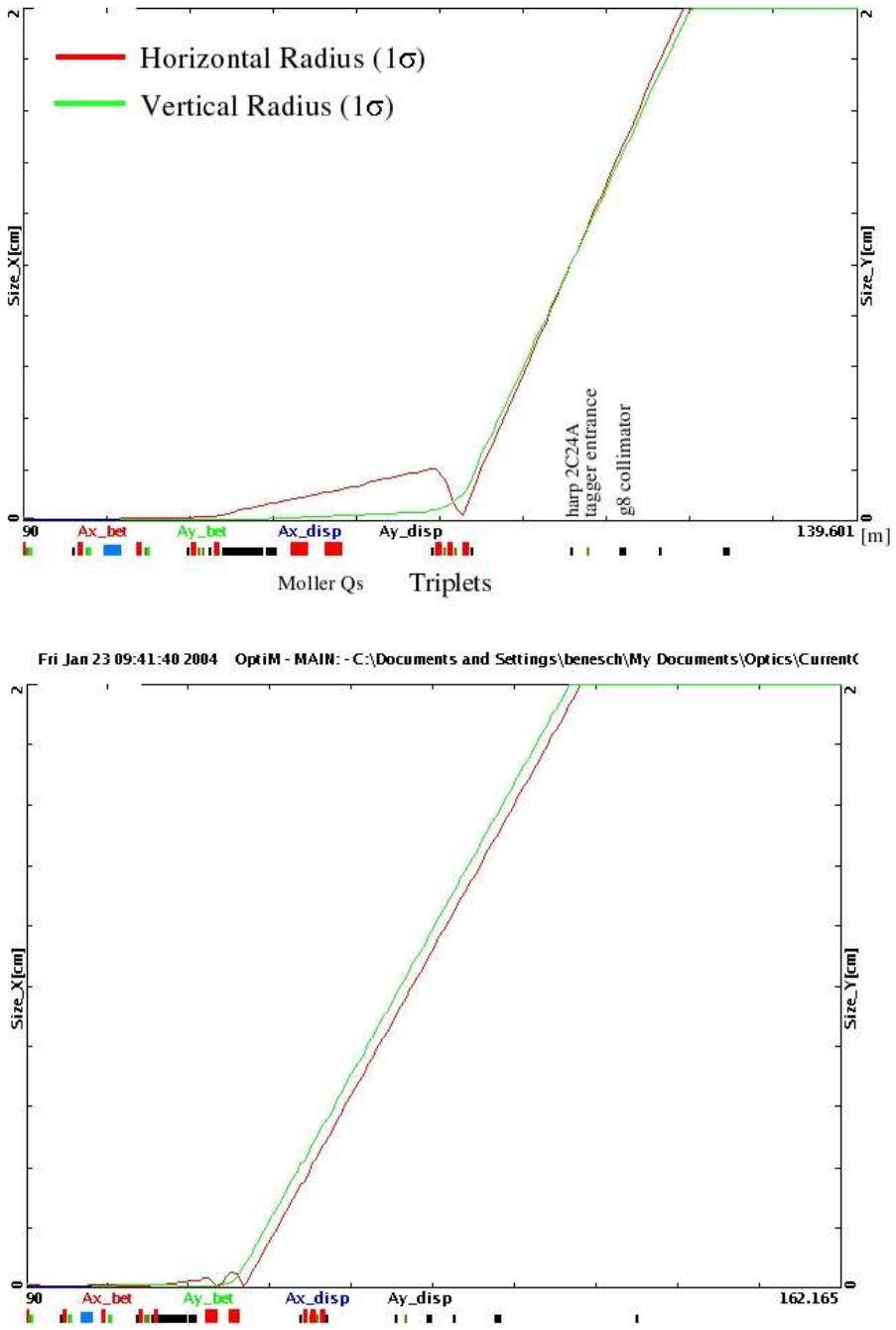

Figure 4: The OPTIM simulation to enlarge the beam spot size using existing beam tranport magnets in hall-B beam line upstream of the tagger. The red and green curves show the 1σ horizontal and vertical beam spot sizes. (top) with out Moller quadrupoles (bottom) with Moller quadrupoles set to 3.5 kGauss.

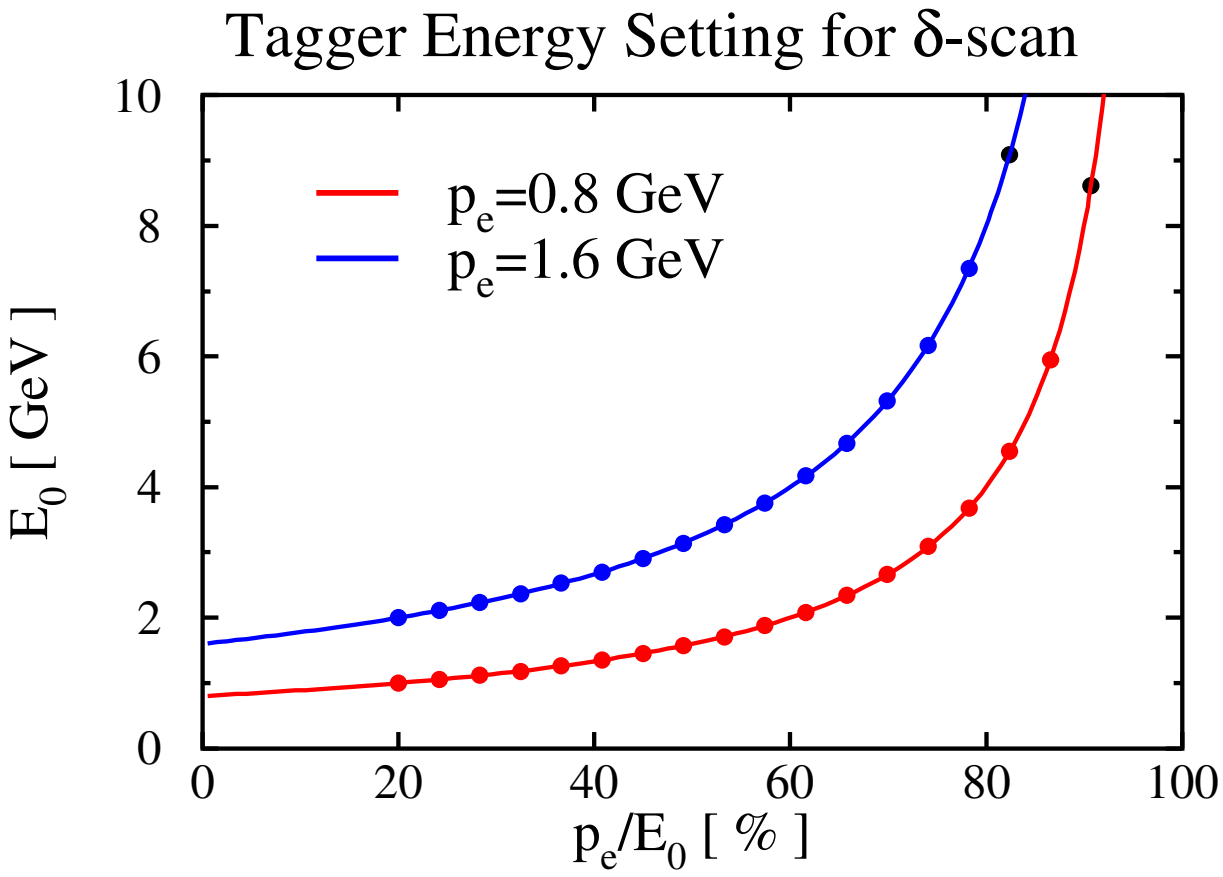

Figure 5: The red and blue curves indicate the field setting of primary electron energy E_0 dependence of the focal plane for post bremsstrahlung electron energies of p_e=0.8 and 1.6 GeV, respectively. Since this calibration is to run without the bremsstrahlung target, p_e represents actually the primary electron beam energy, in this case. Plotted with solid circles are proposed measurement points.